Interplanetary trajectories
Example: Earth to Mars case

Report

Students: Fontanes Molina, Pol; Martínez Viol, Víctor; Urbano González, Eva María

Contents

List of Tables

LIST OF TABLES

List of Figures

1 | Figure example formats

FIGURE

Figure 1.0.1: Landing distance vs MTOW for the Boeing 777.

TABLE

T_1	13 cm
T_2	21 cm
T_3	62 cm
T_t	95 cm

Table 1.0.1: Thickness after the materials correction factor.

2 | Aim

This projects aims to compute an interplanetary trajectory which, for a given ecliptic rectangular positions of two planets in two known time instances, is able to carry a spaceship with a unique impulse, from the first planet to the second.

3 | Theoretical background

3.1 Planetary orbits and approximations analysis

In order to calculate the interplanetary trajectory between two planets, several approximations can be used. The simplest approximation, which can be called *aprox. 0* accepts the following hypothesis:

- Circular and coplanar orbits

- No analysis about the exit of the planet of start is done.

- No analysis about entering the planet of arrival is done.

Aprox. 0 is very basic and can be easily improved adding some parameters.
Another approximation widely used is **Patched Conic Approximation (PCA)**. This method improves significantly the results obtained with *aprox. 0* and represents a good starting point for a more precise numerical analysis of the mission. For this reason, in this project the PCA method will be used.

3.1.1 Patched Conic Approximation (PCA)

The Patched Conic Approximation (PCA) consist on the evaluation of an interplanetary trajectory dividing it into three stages. Considering the Earth as the planet of start, this stages are:

- Geocentric phase: Hyperbolic exit of the Earth. This phase takes place while the probe is going through the influence sphere of the Earth.

- Heliocentric phase: Trajectory with the Sun as main influencer.

- Planet-centred phase: Hyperbolic arrival to the planet of destination. Similarly to the geocentric phase, this phase starts when the probe enters the sphere of influence of the planet.

The influence spheres mentioned are the space close to the planets where it can be considered that the influence of the Sun is negligible in comparison with that of the planet in question. The Laplace criteria will be considered to calculate this sphere. In Table 3.1.1 the radius of the sphere of influence of the solar system's planets are shown.

Planet	$R_I \times 10^6$km	$R_I \times 10^{-3}$ UA	R_I Radius of the planet
Mercury	0.111	0.740	45
Venus	0.616	4.11	100
Earth	0.924	6.16	145
Mars	0.577	3.85	170
Jupiter	48.157	321.0	677
Saturn	54.796	365.3	901
Uranus	91.954	346.4	2025
Neptune	80.196	534.6	3866

Table 3.1.1: Radius of influence of the planets

In order to set out the problem and begin with the resolution of it using the PCA method, the times and positions of the planets at the beginning and end of the trajectory are needed and some hypothesis are taken under consideration. The hypothesis are:

- The spheres of influences of the planets are not considered during the heliocentric phase. This hypothesis is admissible because the radius of the sphere are very small in comparison with the distance between planets.

- The spheres of influence are considered infinite from the point of view of the planet. This is assumed due to the fact that the radius of influence of the planets are much larger than the radious of the planet itself, as can be seen in Tabl 3.1.1.

- The duration of the trajectory can be taken as the duration of the heliocentric phase.

With this data the trajectory can be found through the orbital elements of the trajectories and the thrust required.

3.1.1.1 1st. Geocentric stage

3.1.1.2 2nd. Heliocentric stage

In this section the equations and assumptions done in order to obtain the orbital elements of the trajectory will be explained. The objective of the calculations done regarding this stage is to find:

- Ω : Right ascension of the ascending node.

- e: Eccentricity.

- i: Inclination to the ecliptic plane.

- a: Semimajor axis.

- ω : Argument of the perihelion.

As said previously, the times of departure and arrival are provided, together with the position of the planets. The steps to be followed to achieve the aim of this section are now explained.

Longitude, latitude and distance   The position vector is defined as:

$$\vec{r} = (x_k, y_k, z_k) \tag{3.1.1}$$

Where:

$$x_k = r\cos\beta\cos\lambda \tag{3.1.2}$$

$$y_k = r\cos\beta\sin\lambda \tag{3.1.3}$$

$$z_k = r\sin\beta \tag{3.1.4}$$

Then longitude, latitude and distance are computed with:

$$r = |\vec{r}| \tag{3.1.5}$$

$$\beta = \arcsin\left(\frac{z_k}{r}\right) \tag{3.1.6}$$

$$\lambda = \arctan\left(\frac{y_k}{x_k}\right) \tag{3.1.7}$$

The difference between λ at the beginning and at the end of the trajectory is an important magnitude that will be used. Taking into account that subscript 1 refers to the start position and subscript 2 to the end:

$$\Delta\lambda = \lambda_2 - \lambda_1 \tag{3.1.8}$$

Example: Earth to Mars case   R - 5

Inclination, right ascension of the ascending node and true anomaly variation
Trigonometry has to be used to compute this elements. A general case will be considered, that is to say, that no assumption will be done on whether the two planets are on the ecliptic or not. As shown in reference [1], the equations to be used are:

$$\cos \Delta\theta = \sin \beta_1 \sin \beta_2 + \cos \beta_1 \cos \beta_2 \cos \Delta\lambda \tag{3.1.9}$$

$$\sin A = \cos \beta_2 \frac{\sin \Delta\lambda}{\sin \Delta\theta} \tag{3.1.10}$$

$$\cos i = \sin A \cos \beta_1 \tag{3.1.11}$$

$$\sin l = \frac{\tan \beta_1}{\tan i} \tag{3.1.12}$$

$$\tan \sigma = \frac{\tan \beta_1}{\cos A} \tag{3.1.13}$$

$$\Omega = \lambda_1 - l \tag{3.1.14}$$

Eccentricity, semimajor axis and true anomaly of the starting point With the aim of obtaining this data three equations can be stated. Due to the complexity of the equations, the resolution will be done iteratively. Two cases will be considered: elliptic and hyperbolic. Its equations and iteration process are now shown:

- Elliptic trajectory: The equations of the elliptic trajectory are:

$$e = \frac{r_2 - r_1}{r_1 \cos \theta_1 - r_2 \cos(\theta_1 + \Delta\theta)} \tag{3.1.15}$$

$$a = \frac{r_1 (1 + e \cos \theta_1)}{1 - e^2} \tag{3.1.16}$$

$$t_2 - t_1 = \frac{365.25}{2\pi} a^{\frac{3}{2}} \left(2 \arctan \left(\sqrt{\frac{1-e}{1+e}} \tan \frac{\theta_1 + \Delta\theta}{2} \right) \right.$$
$$\left. - \frac{e\sqrt{1-e^2} \sin(\theta_1 + \Delta\theta)}{1 + e \cos(\theta_1 + \Delta\theta)} - 2 \arctan \left(\sqrt{\frac{1-e}{1+e}} \tan \frac{\theta_1}{2} \right) + \frac{e\sqrt{1-e^2} \sin \theta_1}{1 + e \cos \theta 1} \right) \tag{3.1.17}$$

The iteration process done to solve the equations will deal with the difference between the time of the mission calculated and the real time of the mission, that is a known value. An error criteria ϵ is defined as the convergence value. The flow chart of this iteration is shown in Figure 3.1.1.

Figure 3.1.1: Flow chart for the elliptic trajectory resolution.

- Hyperbolic trajectory: The equations of the hyperbolic trajectory are:

$$e = \frac{r_2 - r_1}{r_1 \cos \theta_1 - r_2 \cos(\theta_1 + \Delta\theta)} \tag{3.1.18}$$

$$a = \frac{r_1 \left(1 + e \cos \theta_1\right)}{e^2 - 1} \tag{3.1.19}$$

$$t_2 - t_1 = \frac{365.25}{2\pi} a^{\frac{3}{2}} \left(\frac{e\sqrt{e^2 - 1}\sin(\theta_1 + \Delta\theta)}{1 + e\cos(\theta_1 + \Delta\theta)} - \right.$$
$$\left. ln \left| \frac{\tan \frac{\theta_1 + \Delta\theta}{2} + \sqrt{\frac{e+1}{e-1}}}{\tan \frac{\theta_1 + \Delta\theta}{2} - \sqrt{\frac{e+1}{e-1}}} \right| - \frac{e\sqrt{e^2 - 1}\sin\theta_1}{1 + e\cos\theta_1} + ln \left| \frac{\tan \frac{\theta_1}{2} + \sqrt{\frac{e+1}{e-1}}}{\tan \frac{\theta_1}{2} - \sqrt{\frac{e+1}{e-1}}} \right| \right) \tag{3.1.20}$$

The resolution is similar to that of the elliptic case, but the acceptable values of the eccentricity change. The flow chart is shown in Figure 3.1.2.

Figure 3.1.2: Flow chart for the hyperbolic trajectory resolution.

Argument of the perihelion   The only remaining orbit element that needs to be computed is ω. It can be calculated using results from the previous steps:

$$\omega = 2\pi - (\theta_1 - \sigma) \tag{3.1.21}$$

3.1.1.3   3rd. Planetocentric stage

4 | Calculations and results

4.1 Verification

In order to verify the code the examples shown at reference [2] will be used. In this section the results provided for every example will be exposed together with the results obtained using the code developed for this project and conclusions will be extracted.

4.1.1 From Earth to Mars using an elliptic heliocentric trajectory

Departure date	2020 Jul 19
Arrival date	2021 Gen 25
Δt	190 days
r_1	(0.4537, -0.9094, 0.0000)
r_2	(0.3148, 1.5078, 0.0239)

Table 4.1.1: Data provided by the first example

Semimajor axis	1.33069 AU
Eccentricity	0.23629
θ_0	359.621°
ω	0.470°
Inclination	1.435°
Ω	296.424º
Heliocentric velocity at departure (km/s)	(29.3678, 14.6982, 0.8229)
Heliocentric velocity at arrival (km/s)	(20.4069,8.2271,0.3656)

Table 4.1.2: Results provided by the first example

Semimajor axis	1.33073 AU
Eccentricity	0.236291
θ_0	359.613°
ω	0.386861°
Inclination	1.43388°
Ω	296.515°
Heliocentric velocity at departure (km/s)	(29.367,14.6986,0.822024)
Heliocentric velocity at arrival (km/s)	(-20.4068,8.27743,-0.364583)

Table 4.1.3: Results computed by the code developed for the first example

Parameter	Relative error (%)
a	0.0030
e	0.0004
θ_0	0.0022
ω	17.6891
i	0.0780
Ω	0.0307
v_{t_1}	0.0017
v_{t_1}	0.0001

Table 4.1.4: Relative error in the first example

4.1.2 From Mars to Jupiter using an elliptic heliocentric trajectory

Departure date	2026 Jun 05
Arrival date	2029 April 25
Δt	1055 days
r_1	(1.3277, 0.4901, 0.0223)
r_2	(5.0135, 2.1380, 0.0505)

Table 4.1.5: Data provided by the second example

Semimajor axis	3.45403 AU
Eccentricity	0.59218
θ_0	350.769°
ω	182.312°
Inclination	7.513°
Ω	207.121º
Heliocentric velocity at departure (km/s)	(12.5324, 28.6817, 4.1200)
Heliocentric velocity at arrival (km/s)	(1.9715,7.9799,1.0552)

Table 4.1.6: Results provided by the second example

Semimajor axis	3.45405
Eccentricity	0.592181
θ_0	350.469°
ω	196.156°
Inclination	7.508444°
Ω	207.127°
Heliocentric velocity at departure (km/s)	(-19.0894,24.8148,-4.05809)
Heliocentric velocity at arrival (km/s)	(3.83725,-7.26513,1.08284)

Table 4.1.7: Results computed by the code developed for the second example

Parameter	Relative error (%)
a	0.0006
e	0.0002
θ_0	0.0000
ω	7.5936
i	0.0606
Ω	0.0029
v_{t_1}	0.0014
v_{t_1}	0.0001

Table 4.1.8: Relative error in the second example

4.1.3   From Earth to Mars using an hyperbolic heliocentric trajectory

Departure date	2020 Mar 06
Arrival date	2020 Jun 09
Δt	95 days
r_1	(-0.9609, 0.2466, 0.0000)
r_2	(0.7285, -1.1980,-0.0430)

Table 4.1.9: Data provided by the third example

Semimajor axis	71.08581 AU
Eccentricity	1.01113
θ_0	-53.310°
ω	233.297°
Inclination	2.513°
Ω	345.619º
Heliocentric velocity at departure (km/s)	(9.1364, -41.4090, -1.6612)
Heliocentric velocity at arrival (km/s)	(35.1754,-6.3201,0.1148)

Table 4.1.10: Results provided by the third example

Semimajor axis	71.6165
Eccentricity	1.01105
θ_0	306.691°
ω	233.309°
Inclination	2.51416°
Ω	345.607°
Heliocentric velocity at departure (km/s)	(9.13562,-41.4082,-1.66139)
Heliocentric velocity at arrival (km/s)	(35.1747,-6.31841,0.115199)

Table 4.1.11: Results computed by the code developed for the third example

Parameter	Relative error (%)
a	0.7465
e	0.0079
θ_0	0.0003
ω	0.0051
i	0.0462
Ω	0.0035
v_{t_1}	0.1189
v_{t_1}	0.0028

Table 4.1.12: Relative error in the third example

4.1.4   Verification conclusions

It can be appreciated that in most of the cases the relative error is far less than one. The highest error produced is less than 10%, and its cause probably deal with the equations and assumptions done while computing the results.

The code is taken as valid and can be used in order to obtain other interplanetary trajectory. It has been done in a general manner so the same code can compute elliptic and hyperbolic trajectories with any departure and arrival planet in the solar system.

4.2   Main interplanetary orbit calculations

The cases proposed in reference [2] will be solved.

4.2.1 Case 1: Mars to Jupiter

Departure date	2037 Oct 25
Arrival date	2039 Oct 15
Δt	720 days
r_1	(1.0707, 0.9868, 0.0055)
r_2	(5.2210, 1.4357, 0.1109)

Table 4.2.1: Data provided for case 1

Semimajor axis	4.27012
Eccentricity	0.725509
θ_0	302.422 °
ω	63.3568°
Inclination	2.14985°
Ω	36.89°
Heliocentric velocity at departure (km/s)	(-29.1352,12.6808,1.03727)
Heliocentric velocity at arrival (km/s)	(4.72014,-9.86931,-0.402679)

Table 4.2.2: Results computed for case 1

4.2.2 Case 2: Earth to Mars

Departure date	2033 Mar 13
Arrival date	2033 Aug 05
Δt	145 days
r_1	(0.9848, 0.1338, 0.0000)
r_2	(0.6797, 1.2298,0.0424)

Table 4.2.3: Data provided for case 2

Semimajor axis	1.37053
Eccentricity	0.615632
θ_0	256.507°
ω	103.493°
Inclination	2.15438°
Ω	7.73712°
Heliocentric velocity at departure (km/s)	(-22.8707,24.7746,1.03934)
Heliocentric velocity at arrival (km/s)	(9.73264,-22.7879,-0.898741)

Table 4.2.4: Results computed for case 2

4.2.3   Case 3: Earth to Mars

Departure date	2031 Jan 23
Arrival date	2031 Aug 01
Δt	190 days
r_1	(0.5264, 0.8316, 0.0001)
r_2	(0.0108, 1.4542,0.0309)

Table 4.2.5: Data provided for case 3

Semimajor axis	1.24706
Eccentricity	0.381113
θ_0	282.584 °
ω	77.5612 °
Inclination	2.29274 °
Ω	57.8117 °
Heliocentric velocity at departure (km/s)	(-48.5598,30.3938,2.29362)
Heliocentric velocity at arrival (km/s)	(20.646,-0.03366,-0.70028)

Table 4.2.6: Results computed for case 3

4.2.4   Case 4: Earth to Mars

Departure date	2025 Jul 18
Arrival date	2025 Oct 21
Δt	95 days
r_1	(0.4342, 0.9188, 0.0001)
r_2	(0.6775, 1.3571,0.0118)

Table 4.2.7: Data provided for case 4

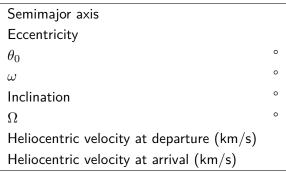|	
Semimajor axis	
Eccentricity	
θ_0	°
ω	°
Inclination	°
Ω	°
Heliocentric velocity at departure (km/s)	
Heliocentric velocity at arrival (km/s)	

Table 4.2.8: Results computed for case 4

4.2.5 Case 5: Earth to Venus

Departure date	2023 May 27
Arrival date	2023 Nov 01
Δt	158 days
r_1	(-0.4255, -0.9194, 0.0000)
r_2	(0.0356, 0.7189, 0.0079)

Table 4.2.9: Data provided for case 5

Semimajor axis	
Eccentricity	
θ_0	°
ω	°
Inclination	°
Ω	°
Heliocentric velocity at departure (km/s)	
Heliocentric velocity at arrival (km/s)	

Table 4.2.10: Results computed for case 5

4.2.6 Case 6: Mars to Earth

Departure date	2033 Jan 18
Arrival date	2033 Aug 28
Δt	222 days
r_1	(1.5831, 0.3913, 0.0306)
r_2	(0.9123, 0.4340, 0.0000)

Table 4.2.11: Data provided for case 6

Semimajor axis	
Eccentricity	
θ_0	°
ω	°
Inclination	°
Ω	°
Heliocentric velocity at departure (km/s)	
Heliocentric velocity at arrival (km/s)	

Table 4.2.12: Results computed for case 6

4.2.7 Case 7: Mars to Earth

Departure date	2030 Nov 20
Arrival date	2031 Jul 06
Δt	228 days
r_1	(1.4166, 0.8722, 0.0530)
r_2	(0.2345, 0.9893, 0.0001)

Table 4.2.13: Data provided for case 7

Semimajor axis	
Eccentricity	
θ_0	°
ω	°
Inclination	°
Ω	°
Heliocentric velocity at departure (km/s)	
Heliocentric velocity at arrival (km/s)	

Table 4.2.14: Results computed for case 7

4.2.8 Case 8: Earth to Mars (hyperbolic)

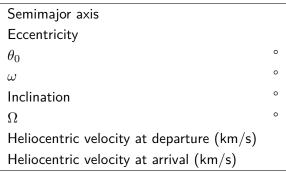|	
Departure date	2021 Nov 26
Arrival date	2022 Feb 19
Δt	85 days
r_1	(0.4383, 0.8843, 0.0000)
r_2	(-0.2082, -1.4582, -0.0255)

Table 4.2.15: Data provided for case 8

Semimajor axis	
Eccentricity	
θ_0	°
ω	°
Inclination	°
Ω	°
Heliocentric velocity at departure (km/s)	
Heliocentric velocity at arrival (km/s)	

Table 4.2.16: Results computed for case 8

4.2.9   Case 9: Earth to Mars (hyperbolic)

Departure date	2022 Jan 15
Arrival date	2022 Apr 20
Δt	95 days
r_1	(-0.4079, 0.8950, 0.0000)
r_2	(0.6393, -1.2542,-0.0420)

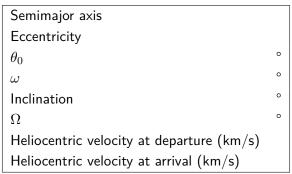Table 4.2.17: Data provided for case 9

Semimajor axis	
Eccentricity	
θ_0	°
ω	°
Inclination	°
Ω	°
Heliocentric velocity at departure (km/s)	
Heliocentric velocity at arrival (km/s)	

Table 4.2.18: Results computed for case 9

5 | Conclusions

6 | Bibliography

[1] J. Calaf, "Trajectòries interplanetàries: Patched Conic Approximation," 2017.

[2] ——, "Treballs de Mecànica Orbital," 2017.

[3] A. Fallis, "Orbital Mechanics for Engineering Students," *Journal of Chemical Information and Modeling*, vol. 53, no. 9, pp. 1689–1699, 2013. [Online]. Available: https://edisciplinas.usp.br/pluginfile.php/66104/mod{_}resource/content/1/ OrbitalMechanicsForEngineeringStudents-AerospaceEngineering.pdf

[4] J. Calaf, "Trajectòries interplanetàries," 2017.